POAC '99
Espoo, Finland

Proceedings of the 15th
International Conference on
Port and Ocean Engineering
under Arctic Conditions

CONSISTENT OBSERVATIONS OF ICE CRUSHING IN LABORATORY TESTS AND FIELD EXPERIMENTS COVERING THREE ORDERS OF MAGNITUDE IN SCALE

R.E. Gagnon
Institute for Marine Dynamics, National Research Council of Canada, St. John's, Canada

ABSTRACT

Observations from in-situ video records acquired during laboratory ice crushing experiments and medium scale indentation tests at Hobson's Choice Ice Island exhibit remarkable consistency. Spalling of ice away from the contact zone produces a sawtooth pattern in the load records and nearly all of the actual movement of the indentor into the ice occurs during the sharp drops in load associated with the spalls. The majority of the load is borne on relatively intact ice (hard spots) where the pressure, from calculations using load data and measured hard spot areas and from pressure sensors, is in the range 40-70 MPa. The visual data show how spalling determines the evolution of hard spot size and shape during the tests. Melt produced in the hard spot areas has been observed in the laboratory tests and its thickness measured. Significant quantities of melt produced in the Hobson's Choice tests have also been documented. All of these observations are consistent with a process of heat generation, and consequent melt production, caused by viscous flow of a thin layer of liquid in the high pressure zones. This process accounts for the bulk of the energy dissipation in the experiments and explains how an indentor can rapidly move forward on hard spots consisting of relatively undamaged ice.

1. INTRODUCTION

Over the past two decades several laboratory and field studies have been conducted to investigate the behavior of ice in impact and indentation situations. Much of this work has been driven by the needs of development of offshore resources in cold ocean environments where sea ice and glacial ice pose serious hazards for ships and fixed and moored floating structures. Some of the research has also been directed towards installation and operation of bridges. Whatever the scenario, it is important to understand the ice behavior so that global loading can be estimated, and equally important, the distribution of pressure within the area of contact ascertained for design purposes. A number of the studies included documentation of the physical condition of the ice after the experiments, and a few studies have reported in-situ visual data of the ice failure process. The latter have provided unique insights into the complex phenomenon of ice crushing and lead to a comprehensive understanding that adequately explains the visual data and also the other instrumental data, that is, ice load and pressure distribution, indentor displacement and surface temperature. This paper describes a model that explains the ice behavior observed in ice crushing experiments I participated in ranging over 3 orders of magnitude in scale, that is, loads ranging from kN to MN and hard spot contact areas spanning ~ 2.5 cm^2 to 2500 cm^2. Reference will be made to other relevant studies, all of which essentially corroborate with the interpretation given here.

2. DESCRIPTION OF THE EXPERIMENTS

Three different apparatus are described here; two were used in a cold room environment in experiments on freshwater ice and were small scale, whereas the third was a medium scale indentation apparatus used during tests on multiyear sea ice at Hobson's Choice Ice Island.

The first apparatus was designed to measure crushing friction between ice and a rotating steel wheel (Fig. 1). The apparatus consisted of an ice specimen holder supported by an actuator which crushed ice by pulling specimens onto the outer surface of the hydraulically-driven rotating wheel. The wheel was kept stationary in the tests referred to here (Gagnon and Mølgaard, 1991) so that it essentially served as an indentor with slight curvature. The specimen holder had a hole machined through the bottom. Specimens were mounted on a thick glass plate and positioned with the plate in the bottom of the specimen holder so that a video camera could view through the hole, thereby providing visual access through the glass plate and clear ice to the ice/indentor interface.

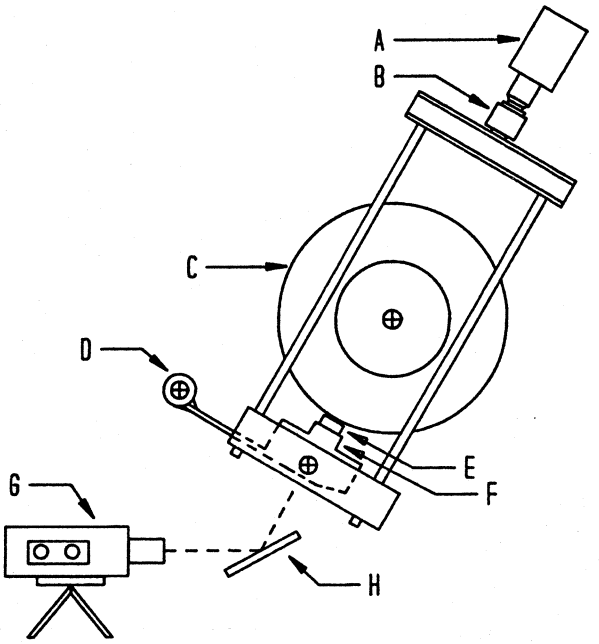

Fig. 1. Crushing friction apparatus: A) hydraulic actuator; B) load cell; C) mild steel wheel (indentor); D) load cell for measuring tension and bending (required in friction experiments); E) ice specimen; F) specimen holder; G) video camera; H) mirror. (From Gagnon and Mølgaard, 1991)

The second apparatus was constructed as a result of the intriguing visual data obtained from the crushing friction apparatus. It used the same visual technique, i.e. viewing through the ice sample, and was designed to provide a wider visual field of view and easier access for illumination. Furthermore the crushing platen was outfitted with pressure sensors, a thermocouple and eventually a liquid sensor so that detailed in-situ pressure, temperature and liquid layer thickness data could be obtained for the ice/platen contact area. Fig. 2 shows the crushing apparatus. Salient features are described here and a detailed description is given by Gagnon (1994a). Ice specimens, confined at the sides by metal plates, sat on a thick transparent Plexiglas plate reinforced with steel to minimize flexure. A mirror was situated at 45^0 between the two load bearing pillars above the Plexiglas plate to permit viewing through the ice specimen to the ice/crushing platen interface. The stainless steel crushing platen is shown in Fig. 3. It had arrays of piston/diaphragm type pressure sensors and thermocouples. At the center of the plate a combined pressure sensor and thermocouple was located to permit simultaneous temperature measurements and pressure measurements at one common point. The electrical connections for the central sensor were modified in the second set of experiments (Gagnon, 1994b) so that the conductance of material over the sensor was measured rather than temperature. In this manner the presence and thickness of a liquid layer was determined.

The ice specimens used in the crushing friction apparatus were large-grained laboratory-grown freshwater samples. Minimizing the number of grain boundaries by having large grains

was desirable in order to reduce the number of cracks at grain boundaries that would obscure the view. The method for growing the large grained specimens was later refined (Gagnon, 1994a) so that single crystal specimens were obtained for the crushing experiments using the second apparatus. The sizes of the ice specimens in tests with the first and second crushing apparatus were similar. The load measurements, visual observations and pressures determined from measured contact areas from the two apparatus were consequently similar. Hence, in the discussion below, the data from the second apparatus will be considered as representative of data from either of the laboratory apparatus. The second apparatus was more advanced then the crushing friction apparatus since it had pressure sensors, thermocouples and a liquid sensor built into the crushing platen. Each sensor was sampled at between 2-21 kHz, depending on the test.

The third apparatus was used for the medium scale indentation experiments at Hobson's Choice Ice Island in 1990 (Masterson et al., 1993). The Ice Island was a 45 m thick floating slab of shelf ice measuring 5 km wide x 8 km long which broke away from the Ward Hunt Ice Shelf in the Canadian Arctic in 1982. The indentation experiments were carried out in a trench (3m x3m x 100m) that had been excavated in one of the 9 m thick expanses of multi-year sea ice attached to the side of the Island. Fig. 4 shows the indentor apparatus in the trench. The walls of the trench were carefully prepared for parallelism, one wall serving as the indentation surface and the other wall as the reaction surface for the back end of the indentor apparatus. The test faces were carved to various shapes to investigate the influence of ice shape on indentation behaviour and to lower the bearing capacity. Test parameters, including ice shape, are given in Table 1. The large scale structure

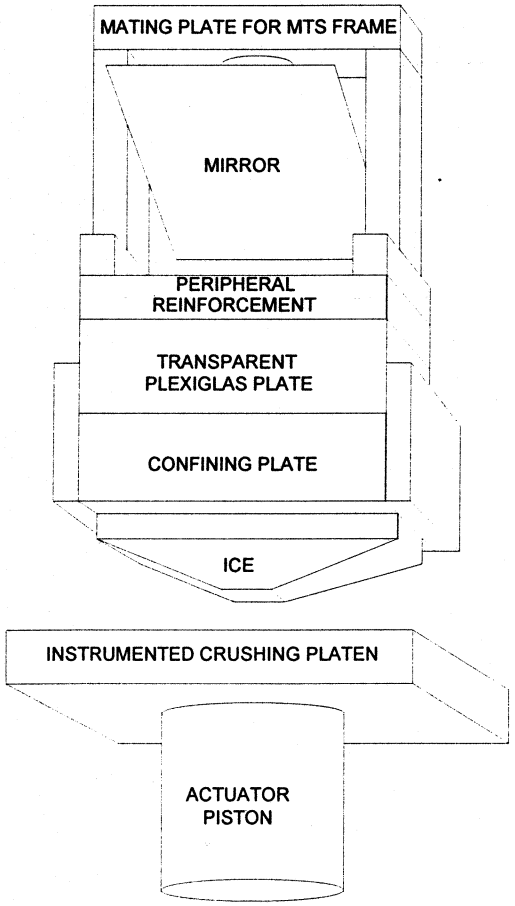

Fig. 2. Crushing apparatus with mirror for viewing the contact zone during experiments. (From Gagnon, 1994a)

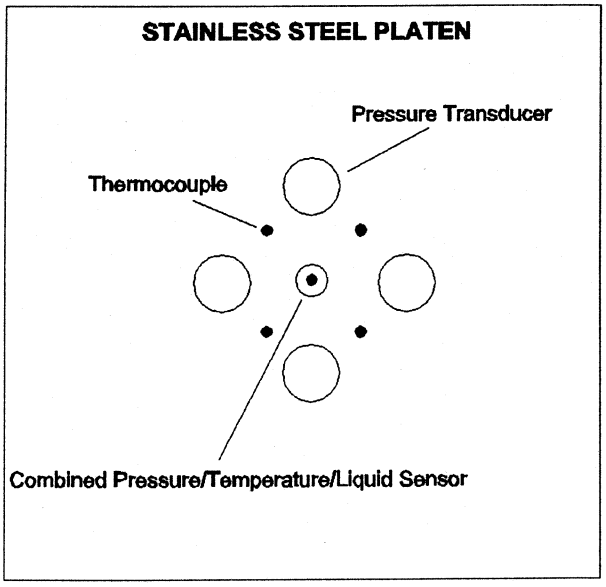

Fig. 3. Stainless steel crushing platen showing the configuration of pressure and temperature sensors and the liquid sensor. (From Gagnon, 1994a)

Table 1. Test matrix for the flat rigid indentor. (From Gagnon, 1998)

Test	Ice Shape	Ice Slope	Initial Contact (mm)	Initial Speed (mm/s)
Tfr1	Vertical wedge	3:1	300	100
Tfr2	Pyramid	3:1	100 x 100	100
Tfr3	Pyramid	3:1	500 x 500	100
Tfr4	Pyramid	3:1	100 x 100	100
Tfr5	Pyramid	3:1	500 x 500	100

of the multi-year ice was rather jumbled due to ridging (Gagnon and Sinha, 1991). The fine structure consisted of snow ice, columnar grained ice (oriented and non-oriented) and frazil ice (oriented and randomly oriented). The ice density varied between 0.875 and 0.886 g/cm^3. The average salinity of the ice at the test faces for the indentation experiments was around 2 ppt.

A variety of indentor shapes were used with the apparatus during the Ice Island test program. The indentor used for the experiments described here, designated as the flat rigid indentor (Tfr), is shown in Fig. 5. It was a 57 mm thick aluminum plate (1.2 m width x 1.5 m height) with a 1 mm thick coating of INERTA. A 35 mm thick Lexan viewing window (300 mm x 150 mm) was located at the center of the plate so that video records of the ice/indentor interface could be obtained during tests. The plate was attached to a rigid mounting pad which in turn was attached to the three hydraulic actuators. The actuators, powered by a bank of accumulators, drove the indentor. Each actuator had a load cell to monitor the force exerted during testing. Displacement of the indentor was controlled using a closed loop system set for a displacement rate of 100 mm/s. The video camera (Sony EVO-9100 Hi8) was installed between the actuators so that it viewed directly through the mounting pad and Lexan

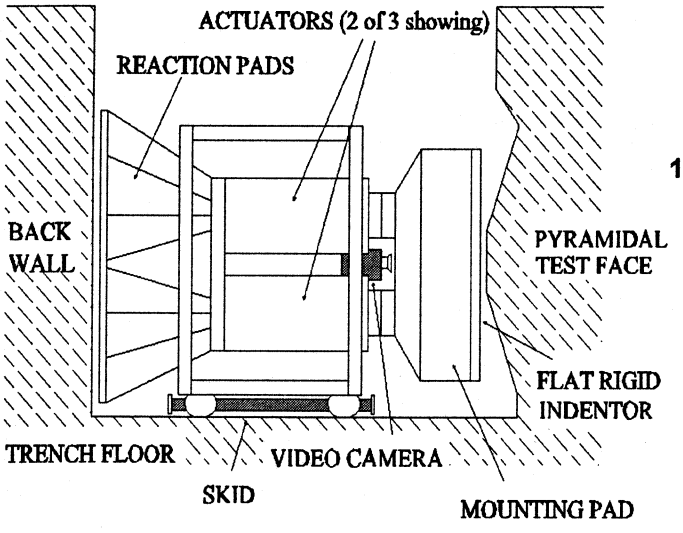

Fig. 4. Schematic of the medium scale indentation apparatus used in the trench at Hobson's Choice in 1990. (From Gagnon, 1998)

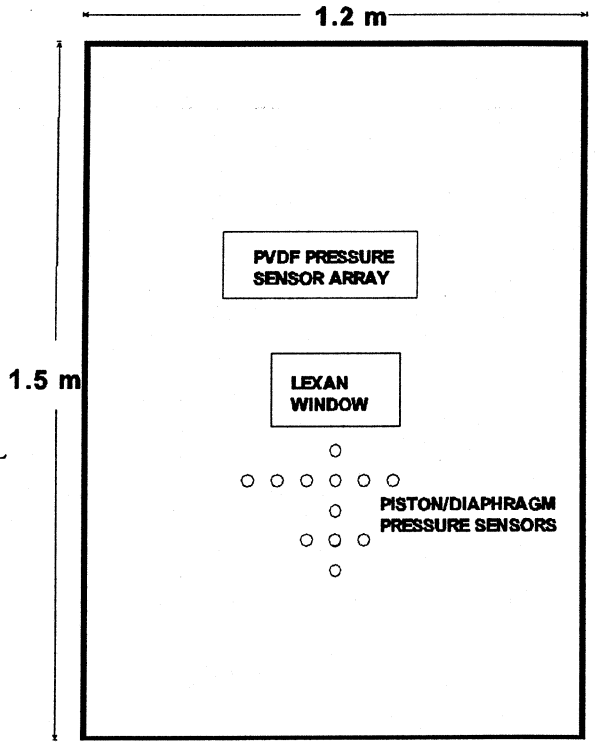

Fig. 5. Frontal view of the flat rigid indentor showing the positions of the viewing window and the pressure sensors. (From Gagnon, 1998)

window. Hence, the viewing technique was somewhat different from the technique used in the first two apparatus since the video camera located inside the Ice Island apparatus viewed the ice/indentor contact from the direction of the indentor, whereas the ice/platen interface was observed through the ice in the other apparatus.

The indentor plate had two types of pressure transducers. A rectangular 26 element (480 mm x 150 mm) PVDF (polyvinylidene difluoride) pressure sensing panel was located above the Lexan window and a series of 12 piston/diaphragm type pressure transducers was situated below the window. A thermocouple temperature sensor was installed in the housing of one of the piston/diaphram type pressure sensors so that the temperature sensing component was flush with the face of the indentor. Data were acquired at 2000 samples per second for each transducer on the apparatus.

3. DATA COMPARISON

In the laboratory and field test programs the data exhibited eight common features. These features are listed as follows, along with references to the work of others where similar observations were made: (1) A sawtooth pattern was evident in the load records (Figs. 6c and 7d) similar to that observed in many ice indentation studies (Michel and Blanchet, 1983; Evans et al., 1984; Määttänen, 1983; Timco and Jordaan, 1988; Sohdi and Morris, 1984; Frederking et al., 1990); (2) When compliance of the ice and apparatus was taken into account it was seen that the majority of the actual movement of the indentor into the ice was not continuos but rather it occurred in rapid jumps corresponding to the sharp drops in load evident in the data records (Figs. 6a and 7a). During load drops the relative velocity of the indentor into the ice in the Hobson's Choice tests was 3-5 times the nominal actuator speed, and in the laboratory tests the crushing platen's speed through the ice at load drops was more than 40 times the nominal actuator speed; (3) During indentation regions of intact ice, relatively small compared to the nominal contact area, were visible in the contact zone surrounded by crushed and damaged ice which moved away from the intact zones (Figs. 8 and 9). Similar observations of hard intact ice regions during ice crushing have been reported by others (Riska et al, 1990; Fransson et al., 1991). Thin section analysis from the lab tests confirmed the intact nature of the ice (Fig. 10) and thin and thick sections (Figs. 11 and 12) from the Hobson's Choice tests showed similar features; (4) The pressure on the intact ice zones (hard spots) was very high (40-70 MPa) and changed abruptly to low values at the peripheral boundary between intact ice and the crushed material at the perimeter. Average pressures calculated from load and nominal contact area in the early stages of indentation, from medium scale indentation tests conducted inside a grounded iceberg at Pond Inlet (Masterson et al., 1992), were in the range of the peak pressures reported here. Similarly, the peak pressures from impact tests on freshwater ice (Timco and Frederking, 1993) and iceberg ice (Gagnon and Gammon, 1997) were comparable to the pressures reported here.

Continuing with the observations: (5) Estimates of the pressure on the hard spots calculated from measured areas of the hard spots and the load data corroborated with the data from pressure sensors (Figs. 13 and 14); (6) The shapes of the hard spots were largely determined by the formation of spalls of ice where each spall could be associated with a load drop. Fig. 15 shows two consecutive images from a high speed video record (unpublished) of a test using the crushing apparatus that capture a spall formation. Similarly, Image 8 of Fig. 9 shows a spall formation (dark feature at the left) during an Ice Island indentation experiment. Spencer and Masterson (1993) have investigated pressure aspect-ratio effects associated with spalling events

in the Hobson's Choice tests. (7) When a spall forms the pressure on the remainder of the ice contact suddenly increases (Fig. 6 (b) and Fig. 7 (b, c)); (8) Temperature measurements indicated the production of liquid water at the interface and this was confirmed from post test thin section analysis of ice from the Ice Island (Gagnon and Sinha, 1991) and from direct in-situ measurements of the liquid layer thickness from the laboratory tests (Fig. 16). Melt production during impact tests has been reported by Kheisin and Cherepanov, 1970.

It was noted above that the hard spots bore most of the load during the tests and that they remained in continuos contact with the indentor throughout the experiments while changing shape as ice spalls broke away from their peripheries. These observations raise a question central to understanding the whole process, namely, how is it possible for intact ice to maintain continuos contact with the indentor and yet somehow be removed from the ice/indentor interface

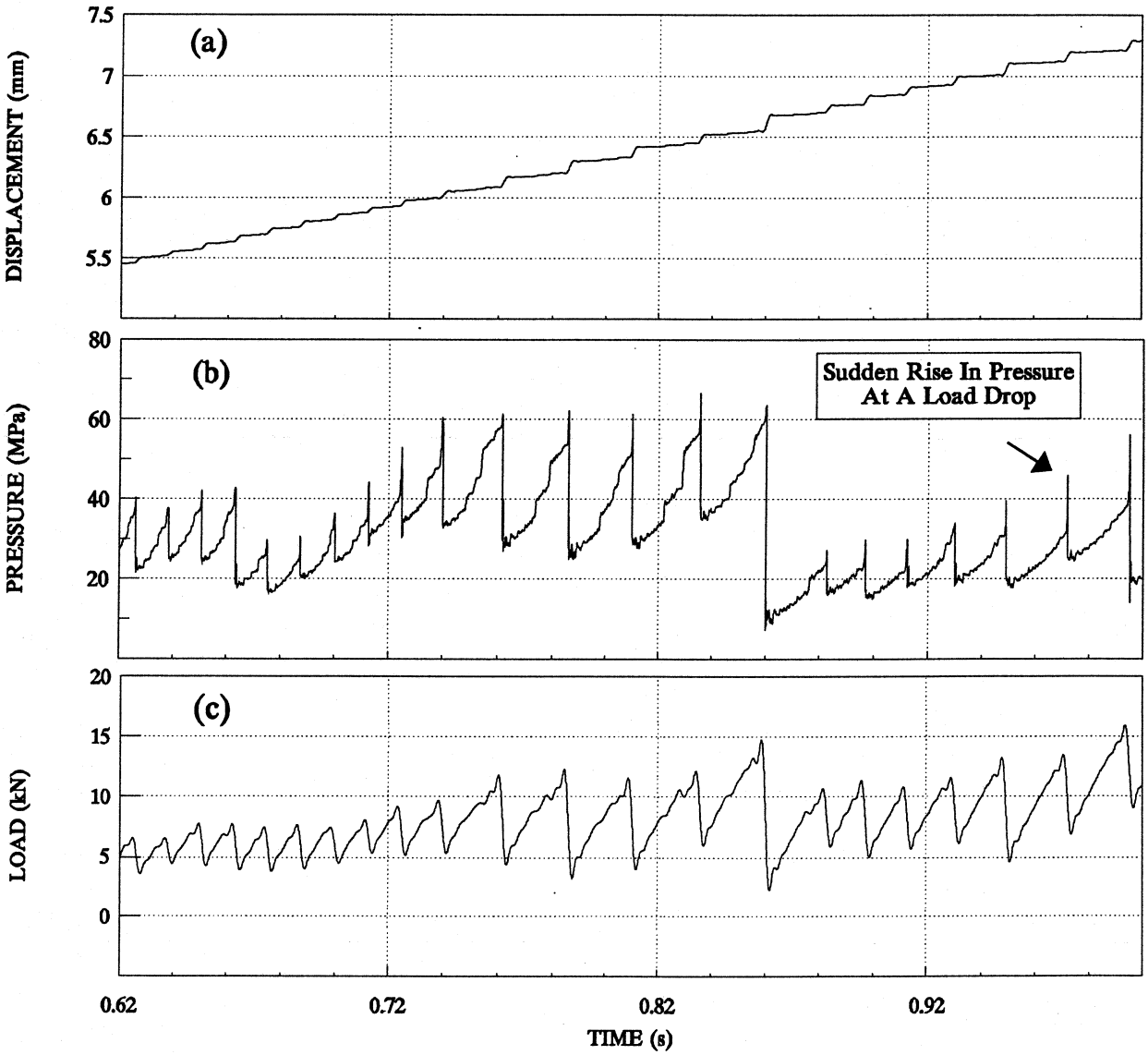

Fig. 6. Sections of the displacement, pressure and load data from a test using the crushing apparatus. (From Gagnon, 1994b)

during the rapid forward movements that occur at the load drops?

A mechanism has been investigated (Gagnon and Mølgaard, 1991; Gagnon 1994a, 1994b; Gagnon and Sinha, 1991) that enables the advance of an indentor, or crushing platen, towards relatively intact ice while maintaining continuos contact, particularly during the rapid forward movement occurring at a spall event. The mechanism accounts for the rapid dissipation of stored elastic energy in the ice/indentor system during load drops through the production and flow of a thin layer of liquid in the high pressure zones. More specifically, when a spall breaks away from the ice contact zone the load is then suddenly borne entirely on the remaining ice (Fig. 17) thereby causing a substantial increase in pressure. In the hard spot region a pre-existing thin layer of liquid on the ice surface (Faraday, 1859), or one that is produced by pressure melting due to the pressure, starts to flow because of the extreme pressure. The viscous flow of the liquid

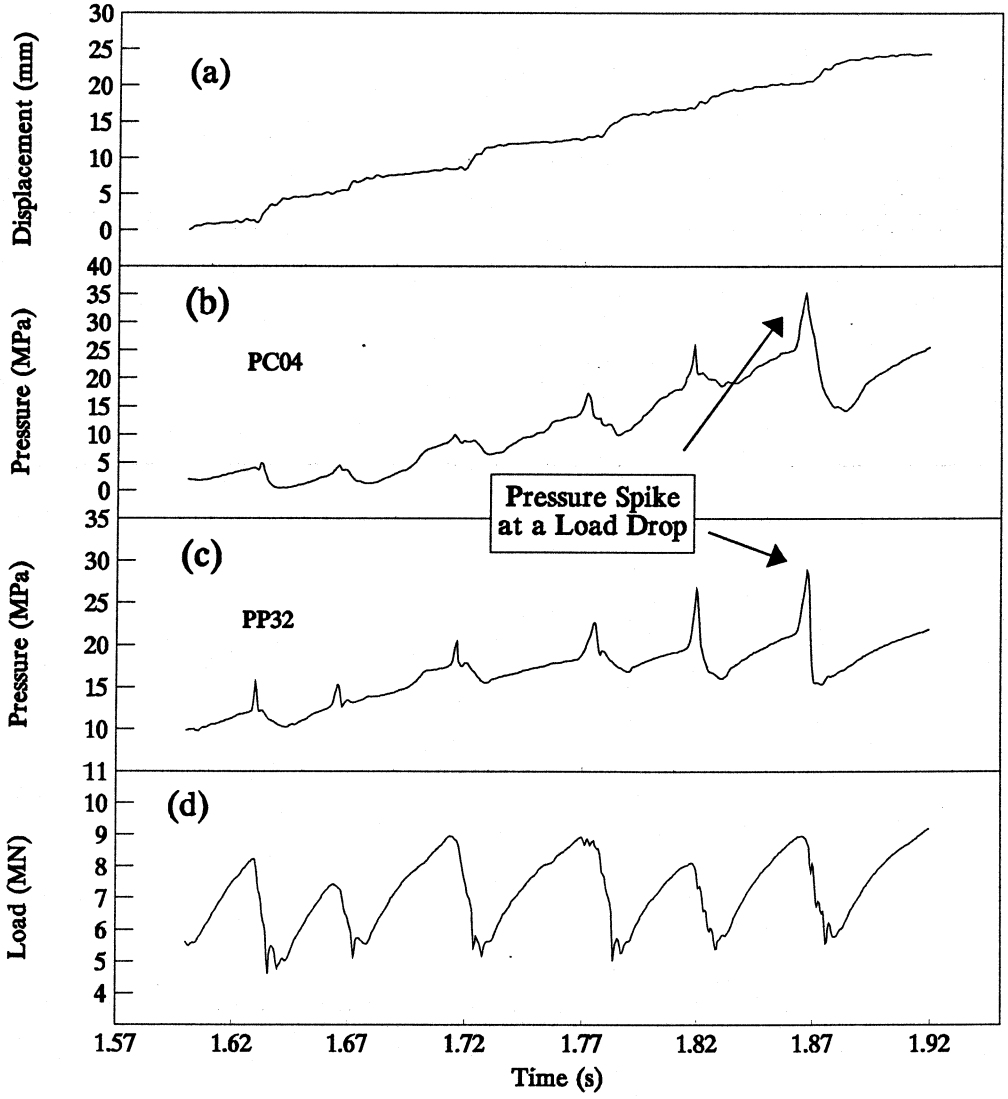

Fig. 7. Time series of displacement (a), piston/diaphragm pressure sensor output (b), PVDF pressure sensor output (c) and load (d) for a segment of Ice Island test Tfr4. The displacement data has not been corrected to account for the ice compliance. The correction would make the gently sloping plateaus almost horizontal. (From Gagnon, 1998)

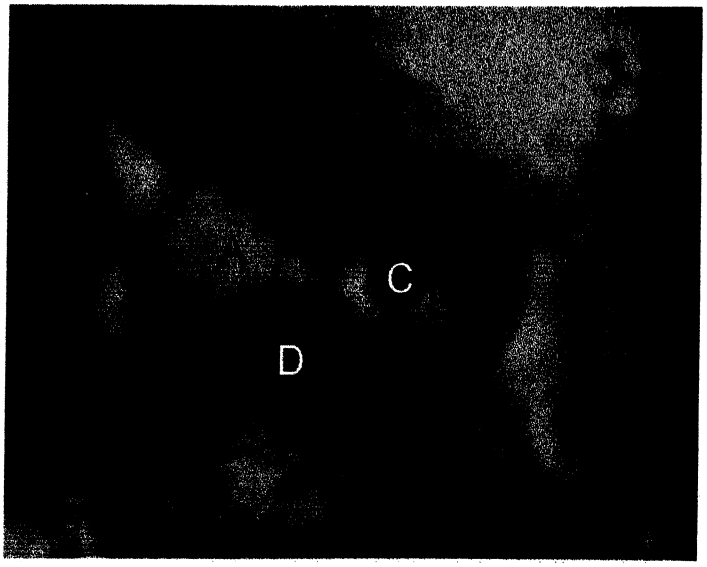

Fig. 8. Video frame showing the platen/ice contact zone during a crushing test. The transparent undamaged zone (A), which covers a fraction of the pressure-sensor piston (B) and marginally encompasses the liquid sensor (C), bears approximately 88% of the load. It is surrounded by opaque material (D) consisting of small ice particles and partially refrozen extruded material from the high-pressure zone. The bright region in the upper right-hand corner is light reflecting internally from the sloping surface of the specimen. The width of the image is 4.6 cm. (From Gagnon, 1994b)

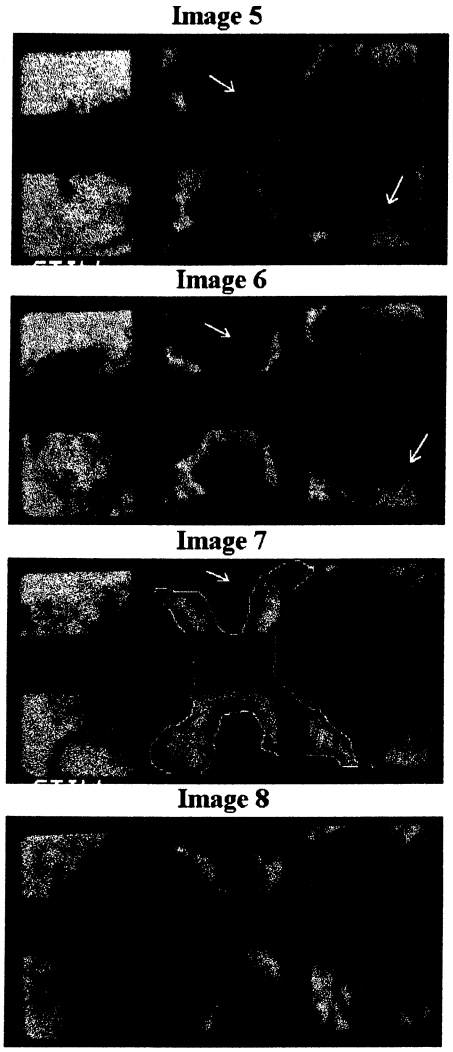

Fig. 9. Four sequential images from early in test Tfr4. The full set of images from the test were acquired at 1/60 s intervals and were numbered starting at 1 for the first image that showed ice contact. The view through the Lexan window was partially obscured by a thick metal grid support. The light 'x' shaped central feature (outlined in image 7) is a hard zone. Arrows point towards features used to track movement of spall debris (dark regions at the sides and top and bottom). The window is 300 mm wide. (From Gagnon, 1998)

Fig. 10. View through crossed-polarized filters of a vertical thin section (light area) taken through a hard spot remnant from an ice sample tested in the crushing apparatus. Apart from a vertically oriented crack, which occurred during unloading, the ice is macroscopically undamaged in the central region (A). The accumulation of dark material at the sides (B) corresponds to the opaque snow-like material surrounding the transparent hard spots in the video records. The unit on the scale is cm. (From Gagnon, 1994a)

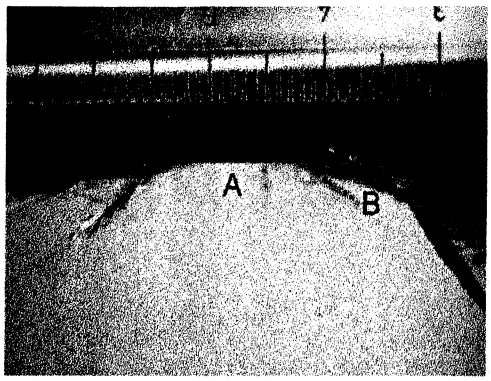

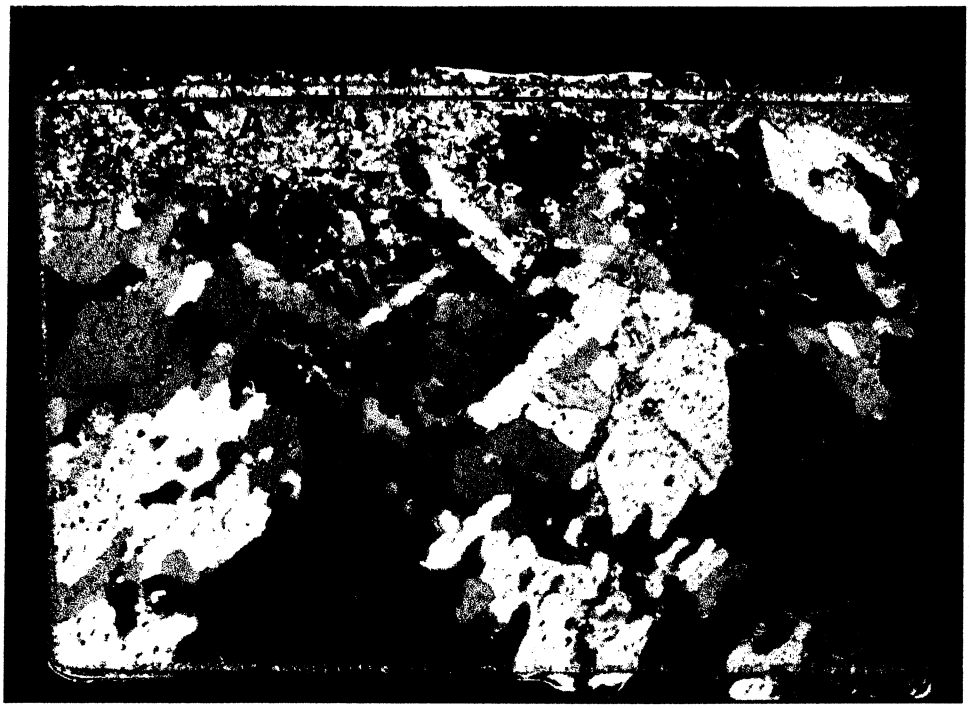

Fig. 11. Horizontal thin section of ice from the hard zone region left on the test face of an Ice Island indentation test. The top of the image corresponds to the ice surface that contacted the indentor. Here a layer of extremely fine-grained ice, varying in thickness from about 1 cm (A) to approximately 1 mm (B) is visible. The dark horizontal line drawn near the top of the thin section corresponds to the boundary between actual tested ice (below the line) and frozen water (above the line) used to bond the thin section to a glass plate. The marks on the scale are millimeters. (From Gagnon, 1998)

Fig. 12. Horizontal thick section from a hard zone left on the test face of an Ice Island test using a different indentor. Crushed ice and possibly refrozen melt, white in appearance, is visible to the sides of the fairly large central region of relatively undamaged ice corresponding to the hard zone. The curved aspect of the contact face was due to the intended flexible nature of the indentor. The width of the image is about 1m. (From Gagnon, 1998)

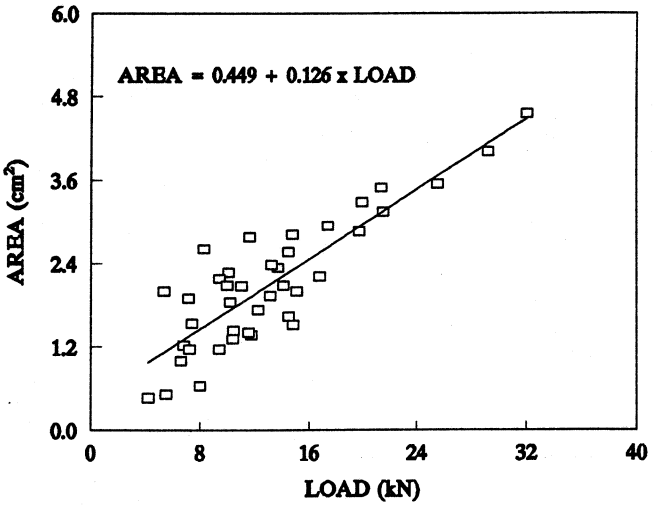

Fig. 13. Transparent contact area versus load for several video frames taken from two tests using the laboratory crushing apparatus at –10°C. (From Gagnon, 1994a)

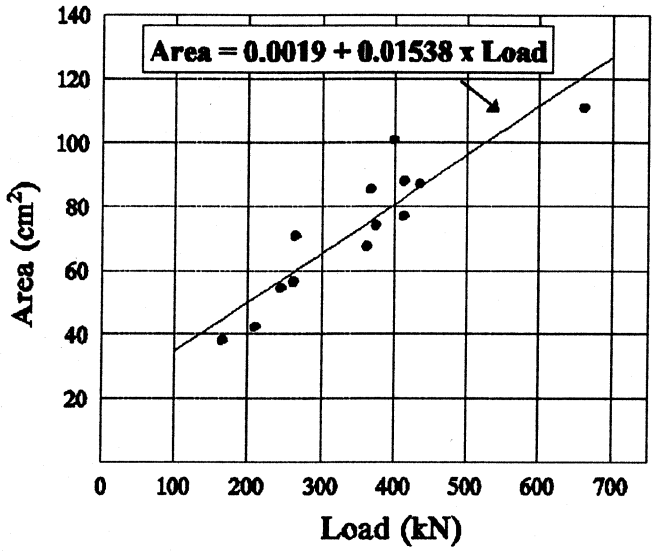

Fig. 14. Hard zone area versus load for several video images taken early in Ice Island tests Tfr2 and Tfr4 conducted at ~ -8°C. The estimated error in the area measurements is ± 15%. (From Gagnon, 1998)

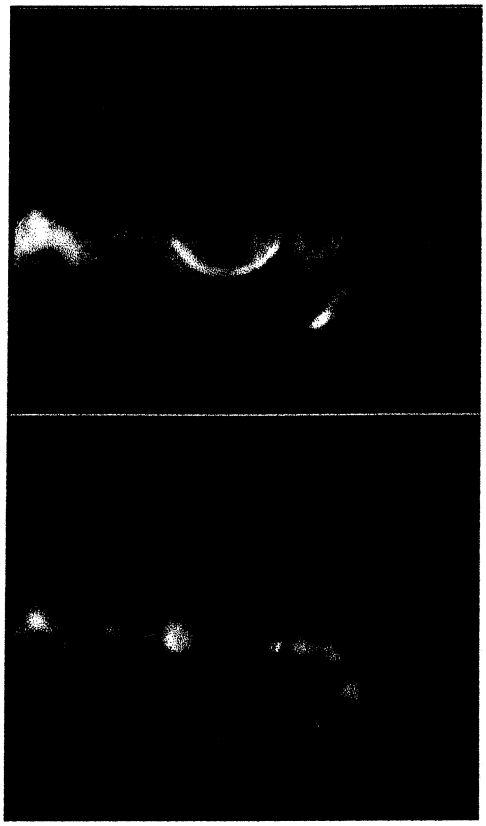

Fig. 15. Two images from a high speed video record of a test using the crushing apparatus that show a spall formation. The top image shows part of the central pressure transducer of the crushing platen viewed through the transparent hard spot. The bottom image was captured immediately after a spall formed and shattered as it broke away from the lower portion of the hard spot. The dark material in the images is a mix of small ice particles from the shattered spalls and partially refrozen extruded material from the high-pressure zone. The images are separated in time by 2 ms.

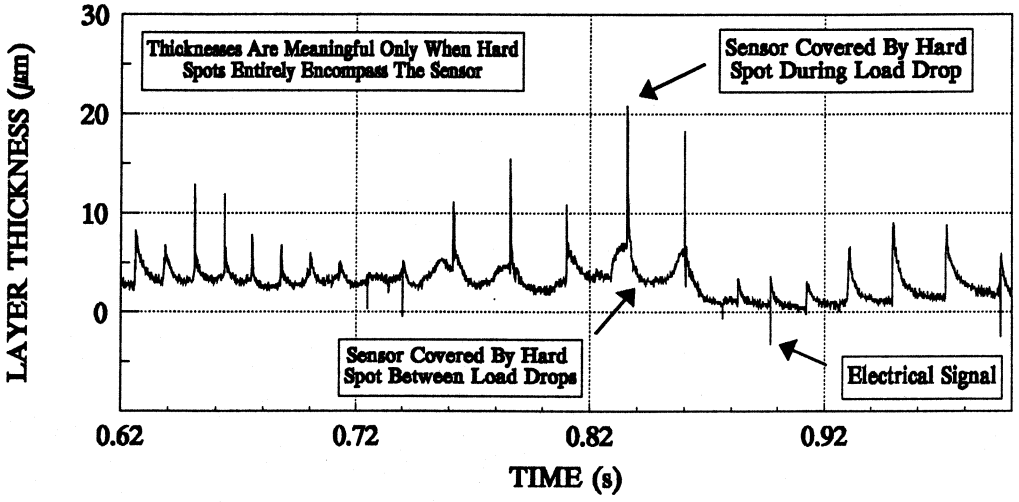

Fig. 16. A section of the liquid sensor data from a test using the crushing apparatus. The test, and time segment, is the same as in Fig. 6. (From Gagnon, 1994b)

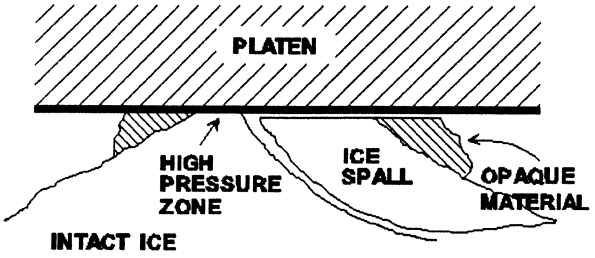

Fig. 17. Schematic of the spalling process that occurs at a load drop. (From Gagnon, 1994b)

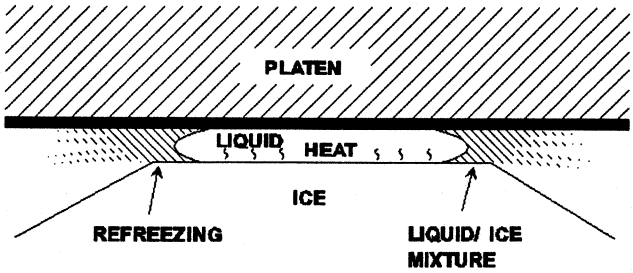

Fig. 18. Schematic of the process of high-pressure viscous flow of melt that occurs when the ice moves against the crushing platen. As determined from data using the laboratory crushing apparatus the relative velocity of the ice towards the platen is ~0.14 cm s^{-1} on the ascending side of a sawtooth in the load record and ~26 cm s^{-1} on the descending side at a load drop. The nominal actuator speed is 0.5 cm s^{-1}. The fluid layer thickness is on the order of μm. A similar scenario is envisaged for larger scale crushing and indentation such as the Ice Island experiments. (From Gagnon, 1994b)

generates heat and additional melting occurs very quickly since the liquid layer is in direct contact with ice, thereby enabling the rapid forward movement of the indentor during load drops while preserving the integrity of the ice in the hard spot (Fig.18). At a load drop the relative movement of the indentor and ice towards each other reduces the stored elastic stress in the ice/indentor system and this lowers the pressure on the hard zone, eventually to the point where the liquid flow process slows considerably or stops i.e. at the bottom of a load drop. Then, as the indentor continues its forward motion towards the ice, load again accumulates until another spall is eventually produced at the contact zone, starting the process over again. Liquid is necessarily produced in the process.

The proposed model for the behaviour of ice during crushing/indentation fits all observations presented here. In summary, it incorporates spalling; it explains the presence of intact hard zones where pressure is high and describes their shape evolution; it relates spalling and load drops to the intermittent rapid forward movements of the indentor; it explains the production of liquid and elevation of temperature at the ice/indentor interface; and ultimately it delineates the process for the dissipation of the bulk of the energy of the system during the interaction.

4. CONCLUSION

A conceptual mechanism to describe ice behavior during impact and indentation has been shown to adequately explain all aspects of data, including visual observations, from crushing and indentation experiments using three different apparatus spanning three orders of magnitude in scale. The compelling evidence presented may encourage other researchers to consider this mechanism as an aid to interpreting ice impact and indentation data.

5. REFERENCES

Evans, A.G., Palmer, A.C., Goodman, D.J., Ashby, M.F., Hutchison, J.W., Ponter, A.R.S. and Williams, G.J. 1984. Indentation spalling of edge-loaded ice sheets. IAHR Ice Symposium, Hamburg, 113-121.

Faraday, M. 1859. On regelation, and on the conservation of force. Phil. Mag. 17, 162-169.

Fransson, L., Olofsson, T. and Sandkvist, J. 1991. Observations of the Failure Process in Ice Blocks Crushed by a Flat Indentor. Proceedings of the 11th International Conference on Port and Ocean Engineering Under Arctic Conditions, St. John's, Canada, Vol. 1, 501-514.

Frederking, R., Jordaan, I.J. and McCallum, J.S. 1990. Field Tests of Ice Indentation at Medium Scale, Hobson's Choice Ice Island, 1989. Proceedings of the 10th International Symposium on Ice (IAHR 90), Espoo, Finland, Vol. 2, 931-944.

Gagnon, R.E. 1994a. Generation of Melt During Crushing Experiments on Freshwater Ice. Cold Regions Science and Technology, Vol. 22, No. 4, 385-398.

Gagnon, R.E. 1994b. Melt Layer Thickness Measurements During Crushing Experiments on Freshwater Ice. Journal of Glaciology, 1994, Vol. 40, No. 134, 119-124.

Gagnon, R.E. 1998. Analysis of Visual Data from Medium Scale Indentation Experiments at Hobson's Choice Ice Island. Cold Regions Science and Technology, Vol. 28, 45-58.

Gagnon, R.E. and Gammon, P.H. 1997. In situ thermal profiles and laboratory impact experiments on iceberg ice. Journal of Glaciology, Vol. 43, No. 145, 569-582.

Gagnon, R.E. and Mølgaard, J. 1991. Evidence for pressure melting and heat generation by viscous flow of liquid in indentation and impact experiments on ice. Proceedings of the IGS Symposium on Ice-Ocean Dynamics and Mechanics, 1990, New Hampshire, Ann. of Glaciol., 15: 254-260.

Gagnon, R.E. and Sinha, N.K. 1991. Energy Dissipation Through Melting in Large Scale Indentation Experiments on Multi-Year Sea Ice. Proc. of the 10th International Conference on Offshore Mechanics and Arctic Engineering, Stavanger, Vol. IV, Arctic/Polar Technology, 157-161.

Kheisin, D.E. and Cherepanov, N.V. 1970. Change of ice structure in the zone of impact of a solid body against the ice cover surface. In Problemy Arktiki i Antarktiki, 34.

Määttänen, M. 1983. Dynamic ice-structure interaction during continuous crushing. CRREL Rep. 83-85.

Masterson, D.M., Frederking, R.M.W., Jordaan, I.J. and Spencer, P.A. 1993. Description of multi-year ice indentation tests at Hobson's Choice Ice Island - 1990. Proceedings of the 12th International Conference on Offshore Mechanics and Arctic Engineering, Vol. 4, 145-155.

Michel, B. and Blanchet, D. 1983. Indentation of an S2 floating ice sheet in the brittle range. Ann. Glaciol., 4: 180-187.

Riska, K., Rantala, H. and Joensuu, A. 1990. Full scale observations of ship-ice contact. Laboratory of Naval Architecture and Marine Engineering, Helsinki University of Technology, Report M-97.

Sodhi, D.S. and Morris, C.E. 1984. Ice forces on rigid, vertical, cylindrical structures. CRREL Rep. 84-33.

Spencer, P.A. and Masterson, D.M. 1993. A geometrical model for pressure aspect-ratio effects in ice-structure interaction. Proceedings of the 12th International Conference on Offshore Mechanics and Arctic Engineering, Vol. 4, 113-117.

Timco, G.W. and Frederking, R.M.W. 1993. Laboratory impact tests on freshwater ice. Cold Regions Science and Technology, Vol. 22, No. 1, 77-97.

Timco, G.W. and Jordaan, I.J. 1988. Time series variations in ice crushing. Proceedings of the 9th International Conference on Port and Ocean Engineering Under Arctic Conditions, Fairbanks, Alaska, 13-20.